Analysis of Thermal-Hydrologic-Mechanical Behavior Near an Emplacement Drift at Yucca Mountain

Jonny Rutqvist[1] and Chin-Fu Tsang

Lawrence Berkeley National Laboratory
Earth Sciences Division, MS 90-1116
Berkeley, CA 947 20
USA

Abstract

A coupled thermal, hydrologic and mechanical (THM) analysis is conducted to evaluate the impact of coupled THM processes on the performance of a potential nuclear waste repository at Yucca Mountain, Nevada. The analysis considers changes in rock mass porosity, permeability, and capillary pressure caused by rock deformations during drift excavation, as well as those caused by thermo-mechanically induced rock deformations after emplacement of the heat-generating waste. The analysis consists of a detailed calibration of coupled hydraulic-mechanical rock mass properties against field experiments, followed by a prediction of the coupled thermal, hydrologic, and mechanical behavior around a potential repository drift. For the particular problem studied and parameters used, the analysis indicates that the stress-induced permeability changes will be within one order of magnitude and that these permeability changes do not significantly impact the overall flow pattern around the repository drift.

Keywords: stress, permeability, thermal, hydrologic, mechanical, repository

[1] Corresponding author, Fax: (510)-486-5686, e-mail: jrutqvist@lbl.gov

1 INTRODUCTION

In the last few decades, extensive scientific investigations have been conducted at Yucca Mountain, Nevada, to explore whether the site is suitable for geological disposal of nuclear waste (Bodvarsson et al., 1999). Comprehensive field investigations have been accompanied with numerical modeling to improve the understanding of processes underlying field observations and to predict future conditions at a potential nuclear waste repository. If constructed, a repository would be located in unsaturated rock, several hundred meters above the groundwater table, at a depth of about 300 meters below the ground surface. From this location, radioactive nuclides could only reach the ground surface through transport with the ambient water flow as a solute. First, the solute would have to migrate several hundred meters downward through unsaturated rock masses along with gravity-driven water flow down to the water table. From there, it would have to be transported over a long distance in the saturated zone to possibly reach a downstream ground surface discharge area or shallow drinking water aquifer.

Calculations of radioactive nuclide transport from a potentially damaged waste canister (in an emplacement drift of the repository) through both unsaturated and saturated fractured rock masses, requires an evaluation of the impact of coupled thermal, hydrologic, and mechanical (THM) processes. Radionuclide transport obviously has a direct and strong coupling with hydrologic processes, because the contaminant can only migrate over long distances with the ambient water flow. The most important effect (potentially) of mechanical processes is an indirect coupling through stress-induced

changes in porosity, permeability, and capillary pressure. Such changes can affect groundwater flow, and hence indirectly, the transport of radioactive nuclides.

In this paper, a fully coupled THM analysis is conducted to investigate the impact of hydromechanical (HM) coupling on the flow around a repository drift at Yucca Mountain. The objective is specifically to provide insight into how drift excavation and heat output from the emplaced waste affect the hydraulic properties of the rock mass and thus affect the magnitude and spatial distribution of percolation flux in the unsaturated zone. For this analysis we use a newly developed simulator TOUGH-FLAC (Rutqvist et al., 2001) for modeling of coupled THM processes under multiphase flow conditions. This analysis consists of a calibration phase and a prediction phase (Figure 1). In the calibration phase, the needed hydromechanical rock mass properties are determined by numerical calibration analysis against several field experiments conducted in the Exploratory Studies Facility (ESF) at Yucca Mountain. In the prediction phase, simulation of THM processes near an emplacement drift of a potential repository is conducted. The result of the THM simulation is compared to the result from a pure TH calculation, thereby enable us to evaluate the impact of the HM coupling (e.g., stress-induced permeability changes).

2 APPROACH

The two computer codes TOUGH2 (Pruess et al., 1999) and FLAC3D (Itasca Consulting Group, 1997) have been coupled together for the analysis of coupled multiphase flow, heat transport, and rock deformations in fractured porous media (Rutqvist et al., 2001).

The TOUGH2 code is designed for geohydrologic analysis of multiphase, multicomponent fluid and heat transport, while FLAC3D is designed for rock and soil mechanics. TOUGH2 has been successfully applied in the Yucca Mountain project to predict temperature and moisture distribution of field experiments, including the Single Heater Test (Tsang and Birkholzer, 1999) and the Drift Scale Test (CRWMS M&O, 2000a). FLAC3D has the capability to analyze coupled hydromechanical and thermomechanical responses of soil, rock, or other types of materials that may undergo plastic flow when their yield limit is reached. The codes are coupled through external modules: one that calculates changes in effective stress as a function of multiphase pore pressure and thermal expansion, and one that corrects porosity, permeability, and capillary pressure as a function of stress (Figure 2). Because these coupling functions are material specific, specially designed coupling modules have been constructed and qualified for Yucca Mountain.

At Yucca Mountain, the two stratigraphic units in which the emplacement drifts may be located (upper middle nonlithophysal (Tptpmn) and the lower lithophysal (Tptpll) units of the Topopah Spring Tuff) are both highly fractured and well-connected (CRWMS M&O 2000b). In these rock units, three dominant sets of fractures are oriented almost orthogonal to each other, two subvertical and one subhorizontal, and the mean fracture spacing is around 0.3 to 0.4 meters (CRWMS M&O 2000c). Previous analysis of thermal-mechanically induced displacements at two major heater tests at Yucca Mountain has shown that mechanical deformations in the rock mass can be reasonably well captured with a linear-elastic or nonlinear-elastic mechanical model (Sobolik et al., 1998

and CRWMS M&O, 1999a). This implies that the bulk-rock mass behavior is essentially elastic, although locally a small slip may occur on fracture planes. Next to the drift wall, on the other hand, more significant inelastic shear slip or tensile fracturing may occur because of the strong stress redistribution and a lack of confinement in that region (Figure 3a).

Because of the high density and connectivity of the fracture network, the conceptual model used is a dual-permeability continuum model with interacting fractured and matrix continua. To couple changes in the three-dimensional stress field to rock mass permeability, a cubic-block conceptual model is utilized (Figure 3b). Using this model, the porosity, permeability, and capillary pressure in the fractured continuum are corrected for any change in the stress field according to:

$$\phi = F_{\phi} \times \phi_i \tag{1}$$

$$k_x = F_{kx} \times k_{ix},\ k_y = F_{ky} \times k_{iy},\ k_z = F_{kz} \times k_{iz} \tag{2}$$

$$P_c = F_{Pc} \times P_{ci} \tag{3}$$

where F denotes various correction factors and subscript i denotes initial conditions. The porosity and permeability correction factors are calculated from the initial and current apertures in fracture set 1, 2, and 3 according to:

$$F_{\phi} = \frac{b_1 + b_2 + b_3}{b_{1i} + b_{2i} + b_{3i}} \tag{4}$$

$$F_{kx} = \frac{b_2^3 + b_3^3}{b_{2i}^3 + b_{3i}^3},\ F_{ky} = \frac{b_1^3 + b_3^3}{b_{1i}^3 + b_{3i}^3}, F_{kz} = \frac{b_1^3 + b_2^3}{b_{1i}^3 + b_{2i}^3} \tag{5}$$

where fractures in fracture sets 1, 2, and 3 are assumed to be equally spaced and oriented normal to x, y, and z direction, respectively, and a parallel-plate fracture flow model (Witherspoon et al., 1980) is adopted. The capillary pressure is corrected with porosity and permeability changes according to the Leverett (1941) function:

$$F_{Pc} = \sqrt{\frac{F_k}{F_\phi}} \tag{6}$$

where,

$$F_k = \sqrt[3]{F_{kx} \times F_{ky} \times F_{kz}} \tag{7}$$

In this study, the current fracture aperture b depends on the current effective normal stress, σ'_n, according to the following exponential function (Rutqvist and Tsang 2001):

$$b = b_r + b_m = b_r + b_{\max}\left[\exp(\alpha\sigma'_n)\right] \tag{8}$$

where b_r is a residual aperture, b_m is "mechanical" aperture, b_{max} is the maximum "mechanical" aperture, and α is a parameter related to the curvature of the function (Figure 4a). This relationship can also be expressed in terms of an initial aperture, b_i and changes in aperture, Δb as:

$$b = b_i + \Delta b = b_i + b_{\max}\left[\exp(\alpha\sigma_n) - \exp(\alpha\sigma_{ni})\right] \tag{9}$$

where σ_{ni} is the initial stress normal to the fractures. This expression can be inserted into Equation (5) to derive expressions for rock mass permeability correction factors in x, y and z directions.

For the linkage function from TOUGH2 to FLAC3D, the changes in effective stress caused by multiphase fluid pressure changes are neglected. This is a reasonable approximation considering that the fracture system is unsaturated, with a capillary

pressure less than 0.01 MPa (Bandurraga and Bodvarsson, 1999), which is several orders of magnitude smaller than the *in situ* stresses and expected thermal stresses at Yucca Mountain. Thus, for the unsaturated zone at Yucca Mountain, mechanical processes such as excavation of drifts and thermo-mechanical processes caused by heating of the rock, can induce rock deformations, while the changes in pore fluid pressure are so small that they could not induce any significant deformations. Because the fractured porous media is always assumed to be in a static equilibrium, the three-dimensional stress field is the equivalent in the fractured and matrix continua. Therefore, a dual continuum model reduces to a lumped fracture-matrix continuum model (equivalent continuum model). Furthermore, the significantly smaller stress-inducted changes in matrix porosity and permeability are neglected in this analysis.

3 MODEL CALIBRATION OF THE STRESS-PERMEABILITY FUNCTION

The parameters in the stress-aperture function (Equation 9) are estimated through numerical back-analyses of several *in situ* tests conducted in the Exploratory Studies Facility, at Yucca Mountain (Figure 1 and 4). This function is uniquely defined by three parameters:

1) The residual hydraulic aperture, b_r

2) The maximum "mechanical" aperture, b_{max}

3) The exponent α

Three measurements in the Tptpmn unit are used to constrain the nonlinear function. The first data point is obtained from the initial hydraulic aperture (back calculated from the

measured initial permeability in the Tptpmn unit) and initial stress (known from *in situ* stress measurements). The second point is obtained from air-permeability measurements conducted at the Drift Scale Test (Figure 4b). In this test, the temperature in the rock increases up to 200 °C, inducing strong thermal stresses, that are expected to compress fractures to a smaller aperture. Air-permeability measurements show that the permeability decreases at most by a factor of 0.1 near the heated drift (CRWMS M&O 2000a). This air-permeability decrease may partly be caused by increased moisture content in fractures and partly by thermo-mechanical fracture closure. A conservative assumption for the THM calculation is to take the measured reduction in permeability to be caused entirely by the thermal-mechanical effect, probably overestimating its impact for conservatism. Therefore, the residual apertures of the three fracture sets were calibrated to limit the permeability changes during closure to 0.1.

A third data point on the stress-aperture curve (Figure 4) is obtained from numerical back-analyses of air-permeability measurements conducted at three excavated niches located in the Tptpmn unit (Figure 1). These tests were conducted to study permeability changes near a drift wall caused by excavation effects (i.e., mechanical unloading of the rock mass near the drift wall causing fracture opening and consequently permeability increase). In the Tptpmn unit, the air-permeability was measured before and after excavation in 0.3-meter packer-isolated sections along three boreholes located about 0.65 meters above the niches (Wang and Elsworth, 1999). The permeability was found to increase by a factor of 1 (no change) to 1,000 (an increase by three orders of magnitude) averaging between one and two orders of magnitude (Figure 4b). It was also found that

permeability generally changes more in initially lower-permeability sections (Wang and Elsworth, 1999). By model calibration against the field tests conducted in the Tptpmn unit, the stress-aperture parameters that govern the mechanical normal closure behavior were calibrated to: b_{max} = 541.6 μm and $\alpha = 1.1\times10^{-6}$ 1/Pa. Using these mechanical fracture parameters, the calibrated stress-aperture function was tested against a niche excavation experiment conducted in the Tptpll unit (Figure 1). In this unit the air-permeability changed upon excavation on average by factor of two to nine above the drift (2 m from the crown) and by a factor of less than two on the side of the drift (1.5 to 2 m from the edge of the drift). Modeling of this niche test was in good agreement with theses experimental results, indicating that the calibrated basic stress-aperture function is valid for both Tptpmn and Tptpll units.

The back-calculated stress-aperture parameters are included in the material properties for the coupled THM simulation listed in Table 1. In the following prediction analysis, the "mechanical" characteristics of the fractures as defined by the parameters b_{max} and α are assumed to be the same for fractures in all rock units, while the initial and residual apertures depend on respective-rock-unit initial permeability.

4 PREDICTION OF THM EFFECTS NEAR A POTENTIAL REPOSITORY

A coupled THM simulation was conducted on a vertical two-dimensional cross section representing the interior of a repository. The model domain is a multiple-layered column extending 717 meters vertically from the ground surface down to the water table. The

vertical layering for the model was chosen to correspond to the vertical contacts at Nevada State Plane Coordinates 170572.39 m (Easting) and 233194.536 m (Northing), with corresponding geologic contacts for the three-dimensional Yucca Mountain UZ site-scale model 1999 TSPA grid (CRWMS M&O 2000d). The ground-surface boundary was set at a constant temperature of 16.1°C, atmospheric pressure and mechanically free, with the water-table boundary at constant temperature of 32.6°C and mechanically fixed. A yearly infiltration rate of 6 mm was applied at the ground surface. Horizontally, by symmetry, only half of the distance between two drifts (40.5 m) was modeled because the drift spacing is 81 m. Thus, the left boundary was at the middle plane vertically through a drift, and the right boundary was at mid-distance between two drifts. Both lateral boundaries of the model were mechanically fixed and closed for heat and fluid flow. A drift of 5.5 m diameter was simulated as being excavated in the Tptpll unit at a depth of about 366 m. The waste emplacement was designed for a high-temperature or above-boiling case, in which a heat input of 1.45 kW/m (initial heat power) of drift was applied with a forced ventilation period of 50 years. During this ventilation period, 70% of the decay heat was removed. The resulting heat power function is presented in Figure 5. In this figure, the initial heat power of 217.5 W/m is calculated as 1450 w/m x 0.3 x 0.5, reflecting removal of 70% by ventilation and the fact that only one half of the canister is included in the half symmetric two-dimensional model. THM parameters for the two most relevant rock units (Tptpmn and Tptpll) are listed in Table1 and 2, including the calibrated parameters α and b_{max} for the stress-aperture function.

4.1 Excavation of the repository drift

The simulation was conducted by first excavating the drift and then emplacing a thermal waste canister into the drift. Excavation of the drift caused stress and permeability changes in the rock mass immediately around the drift. Most changes occured near the top and bottom of the drift, where the permeably increases by about one order of magnitude. Near the springline of the drift, vertical permeability increased while horizontal permeability decreased, resulting in much smaller changes in mean permeability. These responses are consistent with air-permeability measurements at the niches discussed in Section 3.

4.2 Temperature

After emplacement of the waste in the excavated drift, the temperature in the canister and drift wall rouse rapidly and peaked at about 55 years, a few years after the end of the force ventilation period (Figures 5 and 6a). However, as shown in Figure 5, the temperature in the rock mass away from the drift continues to rise and the mid pillar temperature peaks at slightly less than 100°C after 1,000 years. Figure 6b shows that at 1000 years, a substantial zone with temperatures at the boiling point developed and spread upwards towards the Tptpll rock unit located 55 to 90 meters above the repository level.

4.3 Thermal stress and permeability changes

The increased rock temperature caused thermal expansion of the rock mass with accompanying deformations and increased compressive stresses. The compressive

stresses act across fractures, closing them to a smaller aperture with an associated decrease in permeability. At 10 years, this decrease is able to overcome the initial excavation-induced permeability increases, except possibly in areas very close to the crown of the drift (Figure 6a). With time, the zone of decreased permeability propagates farther from the drift, and at 1,000 years it has reached several hundreds meters above the drift (Figure 6b). In Figure 6b, there is a trend of little change in permeability in the Tptpll layer near the drift, to a larger change at 10 to 60 m above the drift, and to the largest change (k_v/k_i is about 0.1) in the layer about 65 to 85 m above the drift (1145 to 1165 m section in the figure). The largest change, at the 1145 to 1165 m level, results from the initially lower permeability of the Tptpmn unit, which is expected to experience a larger permeability change factor.

4.4 Vertical versus horizontal permeability changes

In general, the calculation shows that the vertical permeability (Figure 6) changes much more than the horizontal (not shown), corresponding to the results that horizontal fractures stay open during the entire heating cycle, while vertical fractures tighten to their residual aperture. The horizontal fractures remain open because no significant thermal stress can develop in the vertical direction, on accounts of the free-moving ground surface, and hence, there is a lack of mechanical confinement in the vertical direction. Vertical fractures, on the other hand, close because thermal stresses develop in the horizontal direction as a result of the confinement (no displacement conditions) at lateral boundaries. For example, at 1,000 years, the results show that horizontal stresses have

generally increased from 2.8 to 8.5 MPa at drift-level, while vertical stresses remain almost unchanged.

4.5 Impact on fluid flow field

The saturation and percolation flux distributions at 1,000 years with and without HM coupling are shown in Figure 7 and 8. The main difference in saturation profiles between TH and THM results is the higher saturation in the middle nonlithophysal unit at the 1,145 to 1,165 m level (Figure 7). The liquid flow patterns, on the other hand, are quite similar between the TH and THM cases (Figure 8). One reason for the similarity in the flow pattern is that the reduced permeability is accompanied by a higher relative permeability from the increased liquid saturation, which may have compensated for part of its impact. Another reason may be that permeability reduction is constant horizontally across the flow domain. Since the vertical downward flux cannot flow around regions of reduced permeability, it is thus forced to take the same flow pattern.

5 DISCUSSION OF RESULTS

The results of this model simulation indicate that the magnitude and distribution of percolation flux near a waste-emplacement drift are not significantly affected by stress-induced hydraulic property changes (Figure 8). Because the percolation flux is not significantly affected, the results for this particular problem do not indicate that HM coupling has a significant impact on the repository performance. This result obviously depends on how well we have represented the natural rock responses and especially how well we have represented the stress-induced hydraulic property changes. Two outstanding uncertainties in our modeling are related to inelastic mechanical behavior at the drift wall

and the residual permeability at high compressive stresses. They are discussed in the remainder of this section.

5.1 Drift wall inelastic behavior

After emplacement of waste, a high heat load and strong temperature rise (above 100 °C) will induce mechanical deformations near the drift wall, with associated fracture responses and permeability changes. A general increase in compressive stresses around the emplacement drift will tend to tighten fractures, resulting in a reduction of permeability. However, at the drift wall, high thermal stresses could induce inelastic behavior in the form of shear slip along pre-existing fractures or rock spalling due to development of tensile fractures, which could lead to increased permeability (Figure 3a). Blair (2001) obtained such an inelastic mechanical behavior and permeability increase, using a distinct element modeling approach. Our continuum modeling, on the other hand, did not indicate any significant inelastic shear or tensile failure at the drift wall, and consequently the permeability did not increase during heating. These apparent differences in model results can be explained by a distinct element model providing more freedom of loose block movements against the free wall surface, while such discrete movements are prevented in the continuum model. Furthermore, the material properties used in the two approaches are difficult to compare and there are considerable uncertainties in the estimate of for example the rock mass strength parameters. In this study the rock mass cohesion (2.6 MPa) and friction angle (57 °) are estimates based on empirical rock engineering relationships (taking into account the intact rock strength and the degree of fracturing, etc). Blair (2001), on the other hand, uses joint cohesion (0.09 MPa) and

friction angle (41 °) which are consistent with the discrete element model used. A detailed modeling of the ongoing Drift Scale Test is beneficial to further calibrate and constrain the rock mass strength properties and reduce uncertainties for the modeling of drift-wall behavior. However, while modeling results at the drift wall are uncertain, our results away from the drift agree with distinct-element modeling results by Blair (2001) and is also confirmed by observations at the Single Heater Test and the ongoing Drift Scale Test conducted at Yucca Mountain. These tests shows very little evidence of inelastic rock mass behavior, and during heating the permeability is generally decreasing (Tsang and Birkholzer, 1999, Sobolik et al., 1998, CRWMS M&O, 1999a, CRWMS M&O 2000a).

5.2 Residual permeability at high thermal stress

In the longer term, at 1,000 years, our modeling shows that permeability decreases significantly in an area extending hundreds of meters above and below the drift (Figure 6b). The model simulation shows that the permeability decreases most in the vertical direction, by closure of vertical fractures. Such closure of vertical fractures has also been confirmed in calculations by Blair (2001), using the alternative distinct-element approach. Our calculated magnitudes of permeability decrease—a factor of 0.1 in the upper non-lithophysal and 0.6 in the lower lithophysal (Figure 6b)—is strongly dependent on the residual fracture permeability. The residual fracture permeability was estimated from measurements at the Drift Scale Test, where a reduction of air-permeability values to 0.1 of their initial values was observed. As discussed in Section 3, this reduction could result from a combination of TM effects and relative

permeability change with saturation. Although attributing all reduction to TM effect appears to be a "conservative" limit for the THM evaluation, considerable uncertainties still linger regarding this parameter. A re-evaluation of field observations at Yucca Mountain, using the fully coupled model and, in particular, the on-going Drift Scale Test, will be of paramount importance to constrain the stress-permeability function further. Furthermore, detailed air-permeability measurements are proposed at new heater tests at Yucca Mountain, which aim to determine the permeability changes induced by thermo-mechanical loading (stress increase), and in particular they aim to determine residual permeability sustained at high compressive stress.

6 CONCLUSIONS

The following conclusions may be made of the present study:

- A fully coupled THM model has been calibrated against ESF niche and Drift Scale Test data. The calibrated model predicts that during excavation of an emplacement drift located in the Tptpll rock unit, permeability around the mid section is expected to increase by one order of magnitude or more above and below the drift, while permeability on the side of the drift is expected to change much less.

- With waste emplacement and thermal input, thermal stress will reduce permeability all around the drift. Although this reduction is relative to the initial excavation-induced permeability increase, a net permeability decrease occurs after about one year of heating.

- In the longer term, thermo-mechanical effects will cause permeability changes far from the drift. Except in the region very close to the drift walls, there is permeability reduction caused by thermal stress, with the most changes found in vertical permeability. The reduction is a function of initial local permeability values, being larger for initially low values. At 1000 years, vertical fractures are fully compressed, having a permeability approaching their residual value.

- Despite permeability changes by up to one order of magnitude, the analysis indicates that HM coupling have no significant effect on the percolation flux pattern immediately above the drift. Consequently, for this particular problem, the HM coupling has no significant impact on the performance of the repository.

- Fracture stiffness and residual permeability at high thermal stress are two important parameters for the THM analysis, which suggests that additional thermal field tests and a further analysis of Drift Scale Test data are important to increase confidence in these parameter values.

Acknowledgments

Reviews by Dr. Yu Shu Wu, Dr. Steven Sobolik and anonymous reviewers are most appreciated. This work was supported by the Director, Office of Civilian Radioactive Waste Management, U.S. Department of Energy, through Memorandum Purchase Order EA9013MC5X between Bechtel SAIC Company, LLC and the Ernest Orlando Lawrence Berkeley National Laboratory (Berkeley Lab). The support is provided to Berkeley Lab through the U.S. Department of Energy Contract No. DE-AC03-76SF00098.

References

Blair, S., 2001. Calculation of Permeability Change Due to Coupled Thermal-Hydrologic-Mechanical Effects. This reference will be updated when the AMR is completed.

Bandurraga, T.M., Bodvarsson, G.S., 1999. Calibrating hydrogeologic parameters for the 3-D site scale unsaturated zone model of Yucca Mountain, Nevada. J. of Contam. Hydrol. 38 (1–3), 25–46.

Bodvarsson, G.S., Boyle, W., Patterson, R., Williams, D., 1999. Overview of scientific investigations at Yucca Mountain—the potential repository for high-level nuclear waste. J. of Contam. Hydrol. 38 (1–3), 3–24.

BSC (Bechtel SAIC Company), 2001. Drift-Scale Coupled Processes (DST and THC Seepage) Models. MDL-NBS-HS-000001 REV 01 ICN 01. Las Vegas, Nevada: Bechtel SAIC Company. ACC: MOL.200110418.0010.

CRWMS M&O (Civilian Radioactive Waste Management System Management & Operating Contractor), 1999a. Thermal test progress report #2. BABEAF000-01717-5700-00001 REV 00. Las Vegas, Nevada: CRWMS M&O ACC: MOL.19991104.0270.

CRWMS M&O (Civilian Radioactive Waste Management System Management & Operating Contractor), 1999b. *TBV-332/TBD-325 Resolution Analysis: Geotechnical*

Rock Properties. B00000000-01717-5705-00134 REV 00. Las Vegas, Nevada. ACC: MOL.19991005.0235.

CRWMS M&O (Civilian Radioactive Waste Management System Management & Operating Contractor), 2000a. Thermal Tests Thermal-Hydrological Analyses/Model Report. ANL-NBS-TH-000001 REV 00 ICN 01. Las Vegas, Nevada: CRWMS M&O ACC: MOL.20010109.0004.

CRWMS M&O (Civilian Radioactive Waste Management System Management & Operating Contractor), 2000b. Seepage Model for PA including Drift Collapse. MDL-NBS-HS-000002 REV 01. Las Vegas, Nevada: CRWMS M&O ACC: MOL.20010221.0147.

CRWMS M&O (Civilian Radioactive Waste Management System Management & Operating Contractor), 2000c. Drift Degradation Analysis. ANL-EBS-MD-000027 REV 00ICN 01. Las Vegas, Nevada: CRWMS M&O. ACC: MOL.20001103.0004.

CRWMS M&O (Civilian Radioactive Waste Management System Management & Operating Contractor), 2000d. Development of Numerical Grids for UZ Flow and Transport Modeling. ANL-NBS-TH-000015 REV 00 ICN 01. Las Vegas, Nevada: CRWMS M&O ACC: MOL.19990721.0517.

Lee, M.Y., Haimson B.C., 1999. Initial stress in the Exploratory Studies Facility Yucca Mountain, Nevada. *Rock Mechanics for Industry* (Amadei, Kranz, Scott and Smeallie Eds.) pp. 743-750.

Leverett, M.C., 1941. Capillary behavior in porous media. Trans AIME. 142: 341-358.

Itasca Consulting Group, 1997. FLAC-3D Fast Lagrangian Analysis of Continua in 3 Dimensions, Version 2.0. Five Volumes. Minneapolis, Minnesota: Itasca Consulting Group.

Pruess, K., Oldenburg, C., Moridis, G., 1999. TOUGH2 User's Guide, Version 2.0, Lawrence Berkeley National Laboratory Report LBLN-43134, Berkeley, CA.

Rutqvist, J., Wu, Y.-S., Tsang ,C.-F., Bodvarsson, G., 2001. Coupling of TOUHG2 and FLAC3D codes for analysis of multi-phase fluid flow, heat transfer and rock deformation. Submitted for publication, June 2001.

Rutqvist, J., Tsang, C.F., 2001. Stress-permeability functions derived from field tests in fractured rocks. Manuscript in preparation. July 2001.

Sobolik,. S.R., Finley, R.E., Ballard, S., 1998. Post-test comparison of thermal-mechanical measurements vs. analysis for the in-situ single heater test, Yucca Mountain, Nevada. Int. J. Rock Mech. Min. Sci. 35 (4–5) Paper No. 056.

Stock, J.M., Healy, J.H., Hickman, S.H., Zoback, M.D., 1999. Hydraulic fracturing stress measurements at Yucca Mountain, Nevada and relationship to the regional stress field. *Journal of Geophysical Research*, 90, B10 pp. 8691-8706.

Tsang, Y.W., Birkholzer, J.T., 1999. Predictions and observations of the thermal-hydrological conditions in the Single Heater Test. J. of Contam. Hydrol. 38 (1–3), 385–425.

van Genuchten, M. T., 1980. A closed-form equation for predicting the hydraulic conductivity of unsaturated soils. Soil Sci Soc Am J 44: 892-898.

Wang, J.S.Y., Elsworth, D., 1999. Permeability changes induced by excavation in fractured tuff. *Rock Mechanics for Industry* (Amadei, Kranz, Scott and Smeallie Eds.) pp. 743-750.

Witherspoon, P. A., Wang, J.S.W., Iwai, K., Gale, J.E., 1980. Validity of the cubic law for fluid flow in a deformable fracture. *Water Resources Res*. 16:1016-1024.

Table 1. Thermal-Hydrologic-Mechanical Properties used in Simulations.

Type	Property	Tptpmn	Tptpll	Source
Hydraulic properties of the fractured continuum	Initial permeability (m^2)	0.37×10^{-12}	0.24×10^{-11}	Hydraulic properties are extracted from BSC (2001) where the permeability and van Genuchten parameters (van Genuchten, 1980) have been determined by model calibration against field measurements according to Bandurraga and Bodvarsson (1999).
	Initial porosity (-)	0.01	0.011	
	van Genuchten's air-entry pressure (kPa)	1.9	12.1	
	van Genuchten's exponent, *m* (-)	0.6082	0.6111	
	Residual saturation (-)	0.01	0.01	
Hydraulic properties of the matrix continuum	Initial permeability (m^2)	0.41×10^{-17}	0.30×10^{-16}	
	Initial porosity (-)	0.11	0.13	
	van Genuchten's air-entry pressure (kPa)	258.9	155.2	
	van Genuchten's exponent, *m* (-)	0.2915	0.2359	
	Residual saturation (-)	0.19	0.12	
Thermal properties of the rock mass	Wet thermal conductivity (W/m °K)	2.33	1.87	Thermal properties are extracted from BSC (2001) and corrected for lithophysal cavities in the Tptpll unit
	Dry thermal conductivity (W/m °K)	1.56	1.2	
	Specific Heat, J/(kg °K)	948.0	770.5	
Mechanical properties of the rock mass	Young's modulus (GPa)	14.77	14.77	Mechanical properties of the rock mass are extracted from CRWMS M&O (1999b) where the properties were estimated based on laboratory and field measurements and empirical formulas involving a rock mass classification index.
	Poisson's ratio (-)	0.21	0.21	
	Cohesion (MPa)	2.6	2.6	
	Friction angle (degrees)	57	57	
	Dilation angle (degrees)	29	29	
	Thermal expansion coefficient (1/°C)	4.14×10^{-6}	4.14×10^{-6}	
	Tensile Strength (MPa)	1.54	1.54	
Hydro-mechanical properties of the fractured continuum	Initial hydraulic aperture for Equation 9, b_i (μm)	80.0	164.8	Calculated from mean fracture spacing, s and isotropic permeability assuming an ideal cubic block model, leading to the following formula: $b_i = \sqrt[3]{k_i \times 6 \times s}$
	Maximum Joint Closure for Equation 9, b_{max} (μm)	541.6	541.6	Determined by model calibration against air-permeability experiments at Niches and DST (see Section 3).
	Exponent for Equation 9, α (1/Pa)	1.1×10^{-6}	1.1×10^{-6}	

Table 2. Thermal-Hydrologic-Mechanical Initial Conditions used in Simulations.

Parameter	Tptpmn[1]	Tptpll[2]	Source
Vertical stress (MPa)	6.5	8.1	Vertical stress gradient is 0.022 MPa/m and $\sigma_h = 0.35 \times \sigma_v$ which is within range of field measurements by Stock et al. (1985) and Lee and Haimson (1999).
Horizontal stress (MPa)	2.3	2.8	
Temperature (°C)	22.2	23.4	Obtained by an initial steady state flow calculation without waste emplacement and using previously calibrated hydraulic properties.
Fracture liquid saturation (-)	0.044	0.028	
Matrix liquid saturation (-)	0.98	0.94	

1) Initial conditions at mid layer elevation of Tptpmn unit about 70 meters above repository level
2) Initial conditions in Tptpll unit at repository level.

Figure Captions

Figure 1. Schematic of modeling steps with model calibration against several field tests conducted in the Tptpmn and Tptpll rock units and model prediction of THM behavior around a nuclear waste emplacement drift located in Tptpll unit.

Figure 2. Schematic of coupling between TOUGH2 and FLAC3D. In the special case of Yucca Mountain the illustrated transfer of multi-phase fluid pressure from TOUGH2 and FLAC3D is not significant and therefore neglected. Only temperature has to be transferred from TOUGH2 to FLAC3D.

Figure 3. Schematic picture of the fractured rock system near a drift and the conceptual stress permeability model used. The illustrated inelastic zone near the drift wall may or may not exist depending on rock mass strength properties.

Figure 4. Schematic of normal stress versus aperture relation (a) and calibration of stress-permeability function (b).

Figure 5. Evolution of heat power (used in the half symmetric model) from canister and temperature at three points on the level of the emplacement drifts.

Figure 6. Temperature distribution and stress-induced changes in vertical permeability at (a) 10 years and (b) 1000 years after emplacement. Dashed white lines depicts isotherms in degree Celsius.

Figure 7. Distribution of liquid saturation for at 1000 years (a) TH and (b) THM analysis. In the TH analysis the HM coupling (stress induced permeability changes) is not considered.

Figure 8. Distribution of percolation flux at 1000 years for (a) TH and (b) THM analysis. In the TH analysis the HM coupling (stress induced permeability changes) is not considered.

Figure

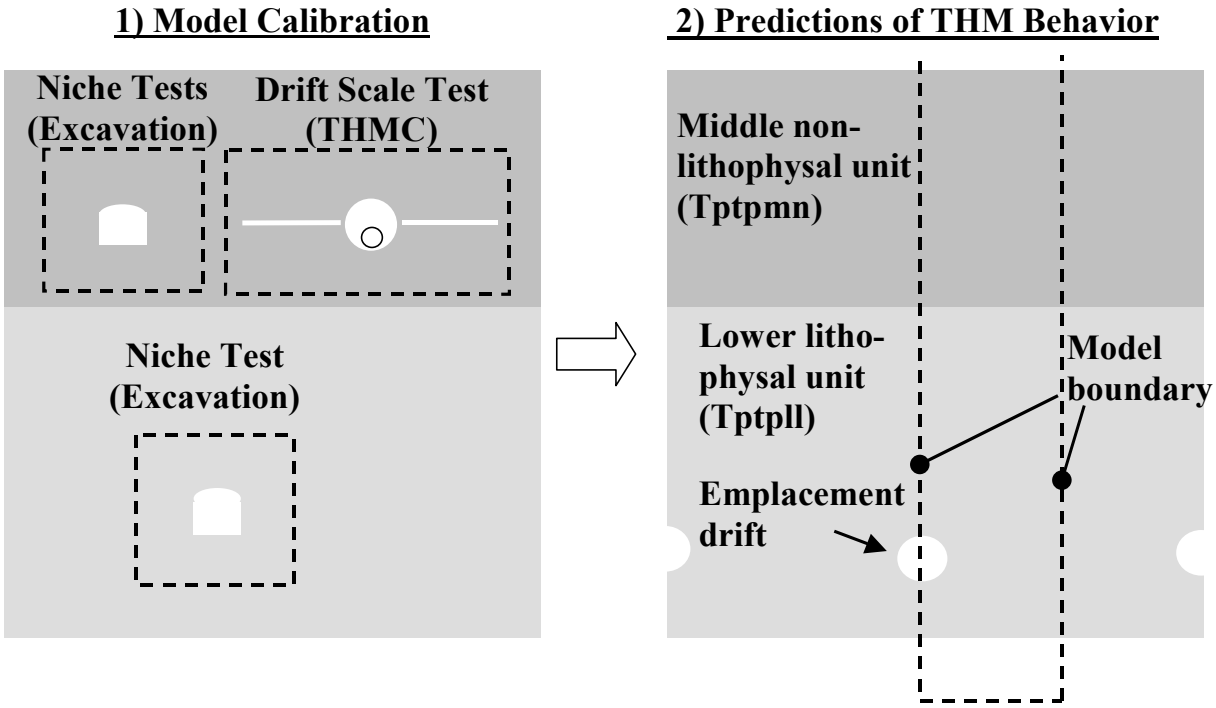

Figure 1. Schematic of modeling steps with model calibration against several field tests conducted in the Tptpmn and Tptpll rock units and model prediction of THM behavior around a nuclear waste emplacement drift located in Tptpll unit.

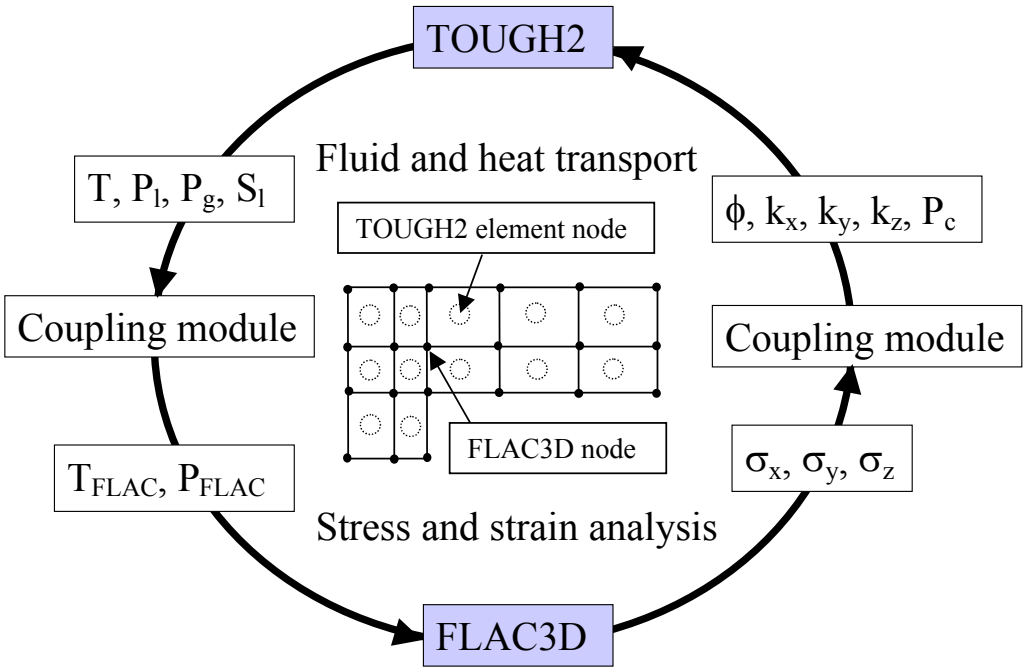

Figure 2. Schematic of coupling between TOUGH2 and FLAC3D. In the special case of Yucca Mountain the illustrated transfer of multi-phase fluid pressure from TOUGH2 and FLAC3D is not significant and therefore neglected. Only temperature has to be transferred from TOUGH2 to FLAC3D.

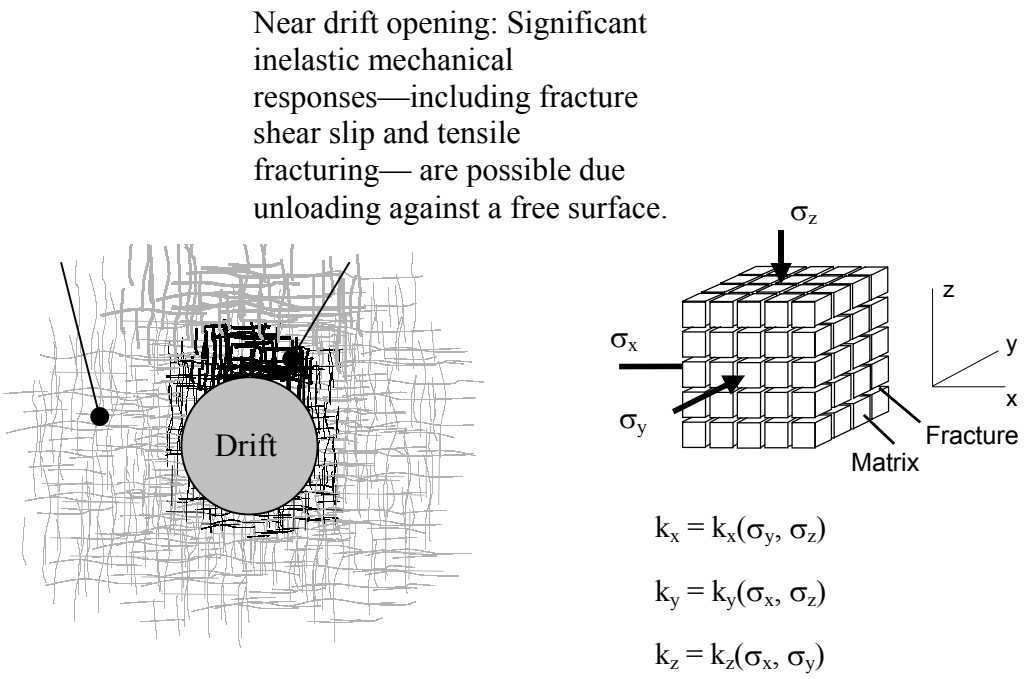

(a) Fractured rock mass system (b) Conceptual stress permeability model

Figure 3. Schematic picture of the fractured rock system near a drift and the conceptual stress permeability model used. The illustrated inelastic zone near the drift wall may or may not exist depending on rock mass strength properties.

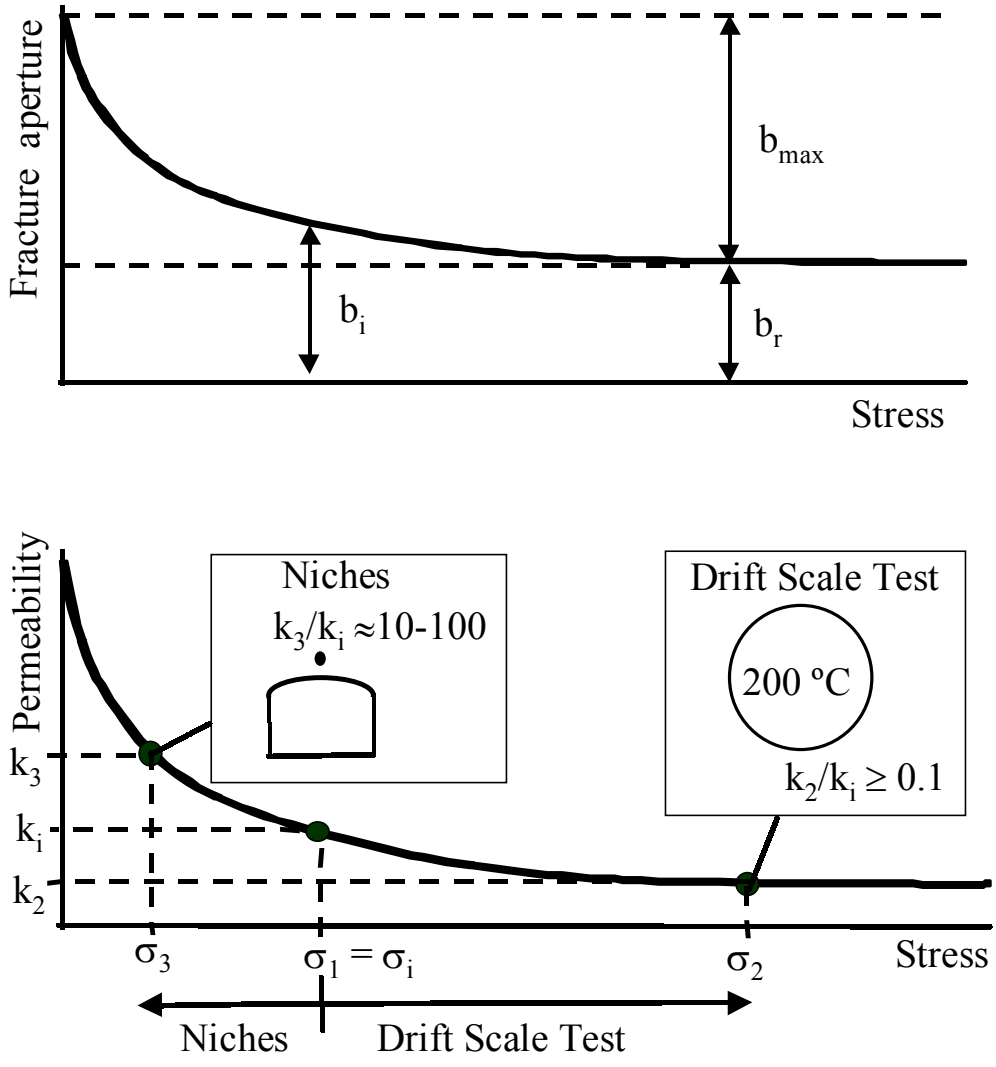

Figure 4. Schematic of normal stress versus aperture relation (a) and calibration of stress-permeability function (b).

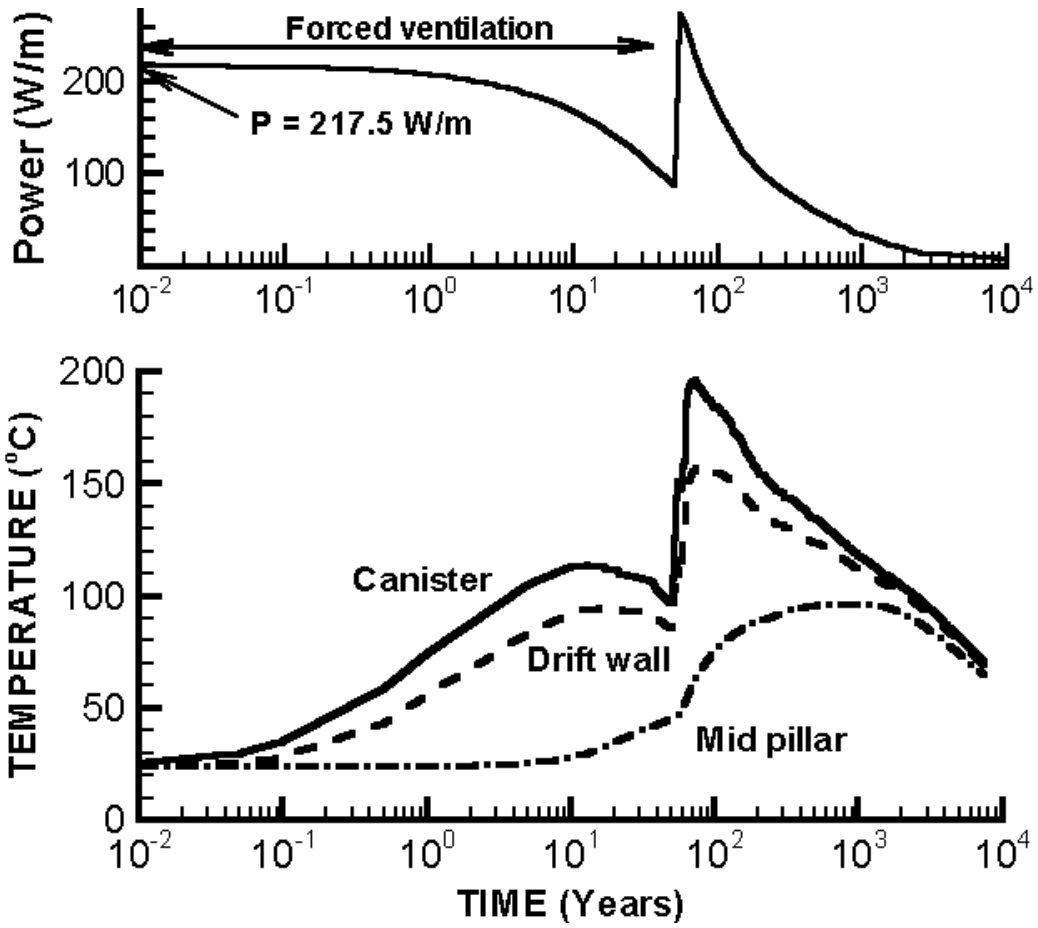

Figure 5. Evolution of heat power (used in the half symmetric model) from canister and temperature at three points on the level of the emplacement drifts.

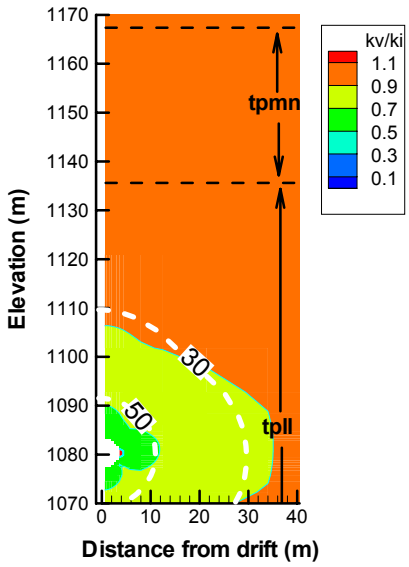

(a)

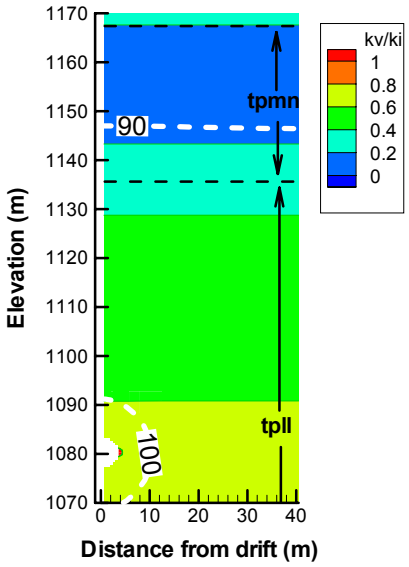

(b)

Figure 6. Temperature distribution and stress-induced changes in vertical permeability at (a) 10 years and (b) 1000 years after emplacement. Dashed white lines depicts isotherms in degree Celsius.

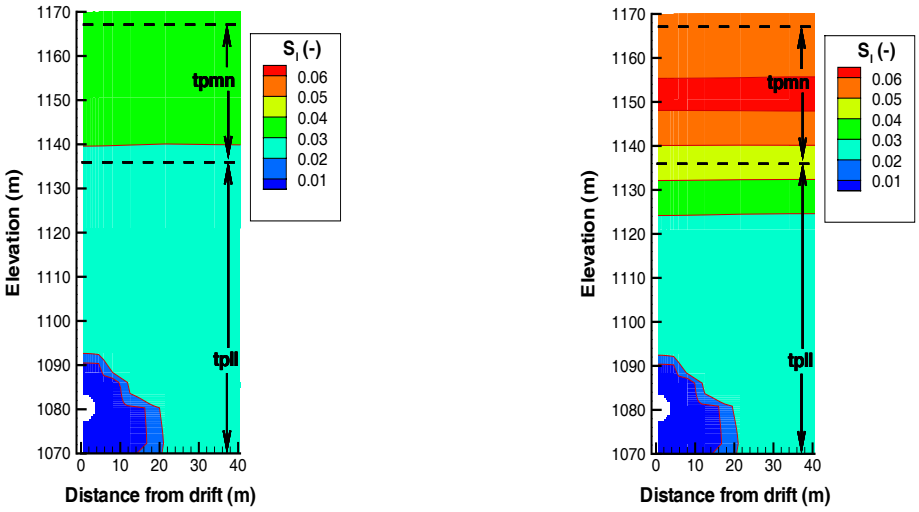

Figure 7. Distribution of liquid saturation for at 1000 years (a) TH and (b) THM analysis. In the TH analysis the HM coupling (stress induced permeability changes) is not considered.

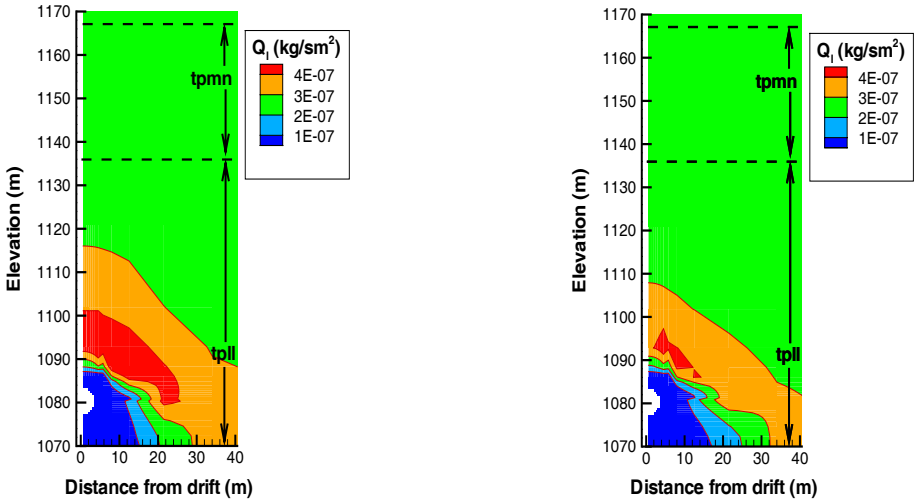

Figure 8. Distribution of percolation flux at 1000 years for (a) TH and (b) THM analysis. In the TH analysis the HM coupling (stress induced permeability changes) is not considered.